Numerical investigation of thermal exchanges for a habitable enclosure in a desert region

A. Oudrane[a,b,*], B. Aour[b] and H. Messaoud[c]

[a]University Center of Tissemsilt (CUT), Road of BOUGARA,
Ben Hamouda, 38004, Tissemsilt (Algeria).
[b]Laboratory of Applied Biomechanics and Biomaterials (LABAB), PBox:
1523 El Mnaour, ENP Oran, 31000, Oran, (Algeria).
[c]Research Unit in Renewable Energies in Saharan Medium (URER'MS),
PBox: 478, Road of Reggane, Adrar, (Algeria).
Tel: +213662830459
[*] **Corresponding Author**: abdellatif.habadat@gmail.com

Abstract

The main objective of this work is to study the thermal exchanges in order to optimize the solar contributions in a habitable enclosure located in a desert region of Algeria (ADRAR). This latter is considered as an air volume of parallelepiped shape limited by horizontal and vertical flat walls, which are the only capacitive elements of the enclosure. They are thermally coupled by conduction, convection and radiation. The external facades of the enclosure are the seat of a convective flux with the external air and radiative exchanges with the environment (ground and sky). Openings (cracks, sealing defects, infiltration orifices, renewal orifices, etc.) allow the air to circulate inside the habitable enclosure and between the inside and the outside. Thermal exchanges are studied using the balance equations established at each wall of the enclosure. These equations are discretized by an implicit finite difference method. The system of algebraic equations thus obtained is solved by the Gauss algorithm using the nodal method. The effects of the outdoor ambient temperature, the density of the incident solar flux and the orientation of the habitable enclosure on the temperatures distributions are analyzed. The evolution of the internal ambient temperature as a function of the wind exposure factor and the degree of leak tightness of the doors and windows is also highlighted at the end of this work. An acceptable agreement was found between the numerical results and those measured by the radiometric station of the ADRAR Saharan Renewable Energy Research Unit. Moreover, the results obtained show that the building material used in this region is the cause of undesirable overheating due to its thermal inertia.

Keywords *Radiation, Habitable enclosure, Nodal method, Thermal exchange, Finite Difference method, ADRAR.*

Nomenclature

α_i	Coefficient of the material absorption	-	Q_{abso}	Quantities of the absorbed heat	W
α_c	Coefficient of the concrete absorption	-	$Q_{solar\ flux}$	Density of solar flux	$W.m^{-2}$
ε_{sky}	Coefficient of the sky emissivity	-	Q_{c_ext}	Amount of heat exchanged by convection with atmosphere	W
λ_c	Concrete thermal conductivity	$W.m^{-1}.K^{-1}$	Q_{iss}	Amount of heat emitted by a surface	W
η_{50}	Hourly rate of air renewal	h^{-1}	$DTFS$	Density of the total solar flux incident on the south wall	$W.m^{-2}$
μ_{air}	Dynamic air viscosity	$Kg.m^{-1}.S^{-1}$	$DTFW$	Density of the total solar flux incident on the west wall	$W.m^{-2}$
ε	Coefficient of exposure to the wind of the heated room	-	S_i	Surface of plan (i)	m^2
ρ_i	Density of the substance (i)	$Kg.m^{-3}$	S_{SFW}	Surface of the wall floor	m^2
Δt	Time difference	s	S_{FS}	Heated floor surface	m^2
Cp_{air}	Specific heat of air	$J.Kg^{-1}.K^{-1}$	S_{small}	Surface of the small opening for introducing air into the heated space	m^2
Cp_i	Specific heat of matter (i)	$J.Kg^{-1}.K^{-1}$	t	Time	s
$C_{inert(i)}$	Inertia capacity of a material (i)	$J.K^{-1}$	T_{A1}	Outdoor air temperature of the habitat	°C
Cp_{WS}	Specific heat of the South wall	$J.Kg^{-1}.K^{-1}$	T_{A2}	Indoor air temperature of the habitat	°C
e_i	Thickness of the material (i)	m	T_{amb}	Ambient temperature	°C
e_{WS}	Thickness of the concrete wall	m	$Tamb(\text{int.})$	Temperature of the internal environment of the building	°C
F_{isky}	Geometric form factor between a surface and the sky	-	T_f	Fluid temperature	°C
g	Constant of gravity	$m.s^{-2}$	T_{gro}	Ground temperature	°C
h_{ci}	Coefficient of convective exchange between the wall (i) and the internal ambient air	$W.m^{-2}.k^{-1}$	T_{HV}	Temperature of the heavens vault	°C
h_{conv}	Convective exchange coefficient	$W.m^{-2}.k^{-1}$	T_i	Temperature of a surface (i)	°C
h_{cv-ext}	Convective coefficient of exchange with the external air of the habitat	$W.m^{-2}.k^{-1}$	T-int	Internal room temperature for a heating slab temperature of 18°C	°C
h_{cviam}	Convective exchange coefficient of ambient	$W.m^{-2}.k^{-1}$	T_{Max}	Maximum ambient temperature	°C

$h_{r-CV.EOW}$	Coefficient of radiation exchange between the celestial vault and the outer west wall	$W.m^{-2}.k^{-1}$	T_{Min}	Minimum ambient temperature	°C
$h_{r-gro.EOW}$	Coefficient of exchange by radiation between the ground and the outer wall	$W.m^{-2}.k^{-1}$	T_S	Temperature of slab heating	°C
$h_{r-gro.ESW}$	Coefficient of exchange by radiation between the ground and the outer south wall	$W.m^{-2}.k^{-1}$	$Tw_{East\ ext.}$	Temperature of the external wall of the East wall	°C
$h_{r-INW.IOW}$	Coefficient of radiation exchange between the north inner wall and the west inner wall	$W.m^{-2}.k^{-1}$	$TW_{East-\text{int}}$	Temperature of the inner wall of the East wall	°C
$h_{r-INW.ISW}$	Coefficient of radiation exchange between the north inner wall and the south inner wall	$W.m^{-2}.k^{-1}$	$Tw_{South-\text{int}}$	Temperature of the inner wall of the South wall	°C
h_{rsky}	Coefficient of exchange by sky radiation	$W.m^{-2}.k^{-1}$	$Tw_{west\ ext.}$	Temperature of the external wall of the West wall	°C
$h_{r-vc.ESW}$	Coefficient of radiation exchange between the celestial vault and the outer south wall	$W.m^{-2}.k^{-1}$	T_{INW}	Internal north wall temperature	°C
m_{SW}	Mass of the south wall	Kg	T_{EOW}	External wall temperature outside	°C
m	Mass of matter	Kg	T_{ESW}	External south wall temperature	°C
m_{air}	Air mass	Kg	V_{tota}	Total volume of the heated space	m^3
m_{WN}	Mass of the northern wall	Kg	V_{wind}	Average wind speed	$m.s^{-1}$

1. Introduction

Over the last ten years, we have witnessed a real enthusiasm for actions to promote high environmental quality. Indeed, the building sector (residential and tertiary) is one of the most energy consuming sectors [1]. However, buildings are designed to act as a thermal filter to recreate an internal microclimate independent of external weather fluctuations. The shape, orientation, arrangement and composition of the components determine the characteristics of this filter. As the inside environment does not always meet the requirements of occupant comfort, the response of the building is corrected by air conditioning units acting as controlled sources of heat or cold and sometimes having an effect on humidity rates [2].

The standards of comfort are still relatively frustrating: an average temperature setpoint to be respected during the heating period, a temperature that should not be exceeded too often during the warm season. These constraints are sometimes refined in detailed specifications, in particular in the case of buildings for individual use [3]. In addition, models describing the thermodynamic behavior of buildings provide a better understanding and design of the passive envelope which allow on one hand to obtain lower energy consumption and greater comfort, and on the other hand to predict the buildings response under extreme situations in order to size facilities and, finally, to assist in the development of new systems or control strategies [2].

The determination of energy consumption in a building may be limited to mass and energy balances, although knowledge of the temperature field and the trend of air movement are necessary for further study [5]. Moreover, these data allow to evaluate the comfort of the occupants (problems of renewal of air, strong temperature gradients, air currents, stratification)

On the other hand, the building is a complex system where many physical phenomena intervene which are usually translated by equations solved using numerical methods. This approach consists in developing models that contribute closely to the development of knowledge and the phenomena quantification. The most well-known model, particularly applied in the building field, is certainly that of Joseph Fourier [6,7]. It characterizes the transfer of heat by conduction in a solid medium. The first motion for resolution, suggested by Joseph Fourier himself, is based on the method of separation of variables. Since this first wall model, Joseph Fourier's experiments on the conduction of iron rings have been replaced by follow-ups of the thermal behavior of whole buildings [7].

The choice of Adrar region is based on the fact that Algeria in particular and the countries of North Africa in general have a great solar potential [8,9]. Solar irradiation rates by satellites of the German Space Agency show exceptional levels of sunshine of the order of 1200 kWh/m^2/year in the northern Great Sahara. On the other hand, the best solar irradiation rates in Europe are of the order of 800 kWh/m^2/year limited to the southern part of Europe [10]. Following a satellite assessment, the German Space Agency concluded that Algeria represents the largest solar potential of the entire Mediterranean basin, ie 169000 TWh/year for solar thermal, 13.9 TWh/year for the solar photovoltaic and 35 TWh/year for wind power. This renewable energy presents currently an adequate solution to the global environmental problems and greenhouse gas emissions that threaten the entire planet. Indeed, it is a sustainable solution to the current energy crisis, with the rise of oil barrel prices. This puts renewable energies (hydraulic, wind, photovoltaic, solar thermal, geothermal, biomass, biogas and fuel cells) at the center of debates on the environment and, more generally, sustainable development.

The concern for rationalizing the use of expensive energies and to design more comfortable buildings has led the various actors in the design and management of buildings to seek better knowledge and control of behavior based on energy optimization of geometric and thermal parameters [4]. In this context, this work is devoted to the development of calculation methods allowing to model the buildings in order to analyze the evolution of its thermal behavior and to foresee the consequences resulting to the response to the excitations applied by its natural climatic environment and the thermal requirements that we must take into consideration [2].

2. Methodology

2.1. Treatment data

In order to assess the energy performance of the building, meteorological data corresponding to a typical year are usually used. This data was used as a reference to compare the behavior of one building to another. These data are usually measured with a one-hour step, but it is possible to have the finer meteorological data, up to the minute [11].

The town of Adrar is located in the south-east of Algeria, about 1540 km from Algiers. The region is characterized by its relatively flat topography, as well as desert geomorphology. In addition, it is characterized by low winter temperatures, high summer temperatures, high sand winds and low atmospheric humidity [12]. The station for measuring climate data (Table 1) is placed at the Renewable Energy Research Unit in the Saharan Environment of Adrar (URER'MS), its geographical coordinates are 27 °, 88'N and -0.27'E, with an altitude of 263m [13].

The available measurements are hourly measurements made during the year 2014 (24 hours per day, 7 days a week). They made it possible to plot the daily variations of the internal and external mean temperatures and the incident solar flux on the walls of the habitable enclosure.

Table 1 Climatic data of Adrar region [13].

Year 2014	June	July	August
Flux_Max (W/m^2)	1052	1051	1040
T_{Max} (°C)	42.2	47.8	47.7
T_{Min} (°C)	25.6	32.5	39.0
Duration of day (h)	14	14	13
Sunrise (h)	5	5	6
Sunset (h)	19	19	19
Wind speed (m/s)	6.8	5.8	6.0

2.2. Descriptive plans of the chamber studied

In the Adrar region, reinforced concrete is the most widely used building material lately due to civilization and because of its rigidity and long life. Figure 1 is a schematic view of a real habitable enclosure that was built by the following elements:

- The exterior walls of the building are constructed using 15 cm thick concrete hollow blocks coated on both sides with a 2.5 cm cement layer;
- The floor is placed on a solid and flat ground with a thickness varying between 10 to 30 cm [14,15]. It is poured directly on the ground. The platform is made of sand, concrete and tiles;
- The roof is composed of hollow concrete bricks, concrete slabs, sand and mortar cement in such a way that the foundations support the loading and shocks.

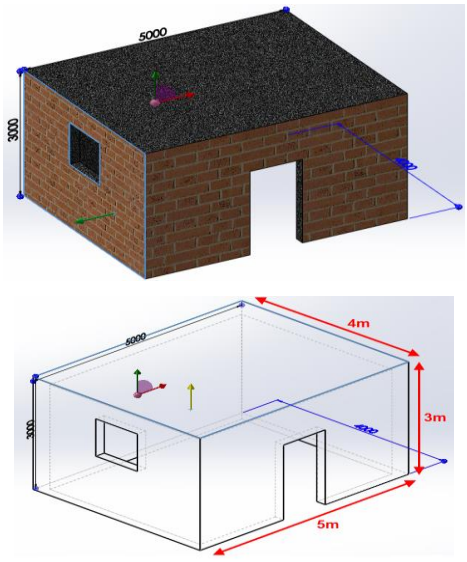

(a) The north and east facades and the outer ceiling

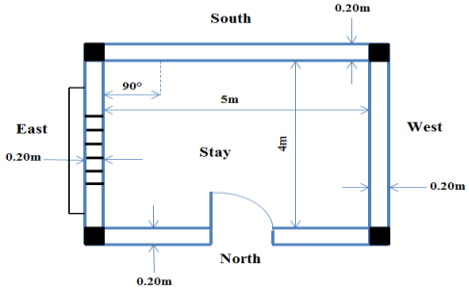

(b) Top view of the habitable enclosure

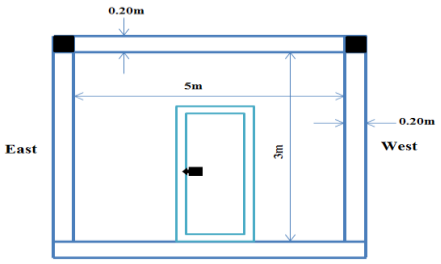

(c) Side view of the north façade

Figure 1 Descriptive plans of the habitable enclosure constructed in Adrar region.

2.3. Physical modeling of thermal transfer phenomena

In the domain of building energy, predictive numerical models have become, in a few years, highly used tools [16]. Thus, simulation models have been developed primarily to meet building envelope sizing needs. These models only concern the thermal exchanges between the ambient and the external facades and the internal ambient with the internal facades of the building walls. In addition, the stratification of the air in an area, the influence of wind on air infiltration, the diffusion of water in the walls, the effect of humidity variations, the changes in state and Latent heat storage are not addressed in this study.

Hence, it is exclusively the envelope that is studied under isotropic conditions. The followed method aims to ensure mastery of basic assumptions and equations and to develop associated modeling aspects (radiation, convection and conduction) [16]. We used the one-dimensional nodal method for the discretization of the energy balances equations which govern these thermal exchanges in the building. The system of algebraic equations thus obtained has been solved by Gauss algorithms.

The proposed mathematical model is based on certain assumptions which can be summarized as follows:

- Thermal transfers through the walls are assumed to be unidirectional and perpendicular to these walls;
- The temperature distribution on the exterior and interior surfaces of the walls is uniform. Therefore, mathematical models will only deliver the average temperatures of the air and walls;
- Modeling is based on the concept of the typical day (Table 2);
- Convection is natural (free) and the flux is laminar;
- The door and the window are assumed to be perfectly closed;
- The heating floor temperature ranges from 18 °C to 28 °C;
- The seventeenth day of July was chosen as a typical day for 2014;
- The outside ambient temperature is equal to the soil temperature $T_{amb} = T_{sol}$;
- It is assumed that the brick is full.

It is worth noting that we have neglected obstacles such as: the cloud, neighboring buildings and trees to be in accordance with the model of Liu & Jordan [17] used in this study. Noting that Campbell & Norman [18] also considered only blue and cloudless skies when calculating the various components of solar radiation. In addition, the solar radiation measurements provided by the Renewable Energy Research Unit in the Saharan environment of Adrar were carried out in an habitable enclosure located in a desert zone with almost the same conditions mentioned above.

Indeed, this method of calculation of solar radiation, proposed by Lui and Jordan, assumes that there is in each month of the year, a typical day or "average day" monthly [22]. In Table 2, we give the numbers of a few typical days in the year starting from January 1, in order to calculate the declination of the sun in the sky and the correction of time.

Table 2 Typical days [19, 20].

Month	''J'' of the month	Typical day	''N°'' Days in the year
June	6	12	163
July	7	17	198
August	8	16	228

Figure 2 shows the different modes of heat transfer at the level of each wall of the habitable enclosure assimilated to a parallelepiped cavity.

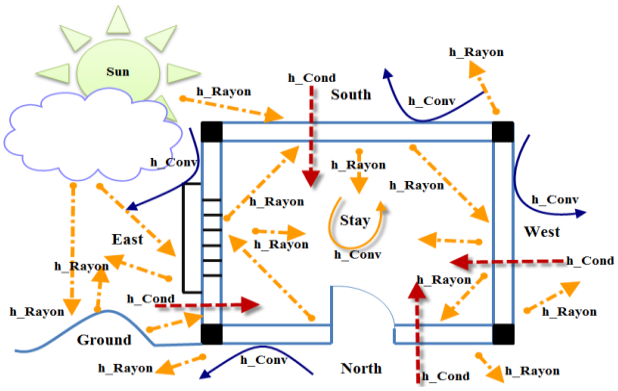

Figure 2 Descriptive diagram of the various modes of heat exchange for the habitable enclosure studied.

The outer wall of the habitat is the seat of a radiative exchange with, on one hand, the celestial vault, and on the other hand, the ambient environment, in particular the soil. The coefficient for determining this transfer is deduced from the following relation [21]:

$$h_{rsky} = \frac{\sigma \times \left(T_{sky} + T_i\right) \times \left(T_{sky}^2 + T_i^2\right)}{\dfrac{1-\varepsilon_{sky}}{\varepsilon_{sky}} + \dfrac{1}{F_{i\,sky}}}; \quad and; \quad T_{sky} = 0.0552 \times T_{amb}^{1.5} \tag{1}$$

Heat exchange between the outer face of the wall and the ambient air is mainly due to wind and it is characterized by the heat transfer coefficient [22, 23]:

$$h_{cv\_ext} = 5.67 + 3.86 \times V_{wind} \tag{2}$$

By considering each wall as an entity independent of the others, it is possible to describe the evolution over time of the thermal transfers in each wall.

In general, the instantaneous variation of the energy within a wall (i) of the model studied is equal to the algebraic sum of the flux densities exchanged with this wall.

The energy balance of the walls of the habitable enclosure is determined by the following government equation [21, 24]:

$$\frac{m_i \times Cp_i}{S} \times \frac{\partial T_i}{\partial t} = DFSA_i + \sum_{i=1}^{n} \times \sum_{x} \varphi_{x_{ij}} \quad (3)$$

where:

$\varphi_{x_{ij}}$ [W.m^{-2}]: Density of heat flux exchanged by the transfer mode x (conduction, convection or radiation) between the media (i) and (j).

$DFSA_i$ [W.m^{-2}]: Density of solar flux absorbed by material (i)

$$DFSA_i = \alpha_i \times \varphi_i \quad (4)$$

φ_i [W.m^{-2}]: Density of solar flux captured by the medium surface (i).

By introducing an exchange coefficient ($h_{x_{ij}}$) and by linearizing the transfers, we can write:

$$\varphi_{x_{ij}} = h_{x_{ij}} \times \left(T_j - T_i\right) \quad (5)$$

Thus equation (3) can be written as:

$$\frac{m_i \times Cp_i}{S} \times \frac{\partial T_i}{\partial t} = DFSA_i + \sum_{i=1}^{n} \times \sum_{x} h_{x_{ij}} \times \left(T_j - T_i\right) \quad (6)$$

with:

$DFSA_i$: Density of solar flux absorbed $\sum \phi_{abso}$.

$\sum_{i=1}^{n} \times \sum_{x} h_{x_{ij}} \times \left(T_j - T_i\right)$: Density of solar flux emitted $\sum \phi_{emit}$.

So, we can write:

$$m_i \times C_{p_i} \times \frac{dT_i}{dt} = \sum Q_{abso(i)} - \sum Q_{iss(i)} \quad (7)$$

We will then apply equation (7) to the various environments of our system. Consequently, the establishment of a thermal balance at each node of the network associated with the habitat model leads to the following transfer equations [25]:

- **Thermal transfer balance at the external south facade**

$$m_{SW} \times Cp_{SW} \times \frac{dT_{ESW}}{dt} = \sum Q_{abso(ESW)} - \sum Q_{iss(ESW)} \quad (8)$$

and;

$$\frac{m_{SW} \times C_{P_C}}{S_{SW}} \times \frac{T_{ESW}^{t+\Delta t} - T_{ESW}^{t}}{\Delta t} = h_{Conv} \times \left(T_{A1}^{t} - T_{ESW}^{t+\Delta t}\right) + \frac{\lambda_C}{e_{SW}} \times \left(T_{ISW}^{t+\Delta t} - T_{ESW}^{t+\Delta t}\right) + h_{r-HV.ESW} \times \left(T_{HV}^{t} - T_{ESW}^{t+\Delta t}\right) + h_{r-gro.ESW} \times \left(T_{gro}^{t} - T_{ESW}^{t+\Delta t}\right) + \alpha_c \times DTFS \quad (9)$$

- **Thermal transfer balance at the internal north façade**

$$m_{NW} \times Cp_{NW} \times \frac{dT_{INW}}{dt} = \sum Q_{abs(INW)} - \sum Q_{iss(INW)} \quad (10)$$

and;

$$\frac{m_{NW} \times C_{P_C}}{S_{NW}} \times \frac{T_{PNI}^{t+\Delta t} - T_{INW}^{t}}{\Delta t} = h_{Conv} \times \left(T_{A2}^{t} - T_{INW}^{t+\Delta t}\right) + \frac{\lambda_C}{e_{NW}} \times \left(T_{ENW}^{t+\Delta t} - T_{INW}^{t+\Delta t}\right) + h_{r-INW.ISW} \times \left(T_{ISW}^{t+\Delta t} - T_{INW}^{t+\Delta t}\right) + h_{r-INW.IEW} \times \left(T_{IEW}^{t+\Delta t} - T_{INW}^{t+\Delta t}\right) + h_{r-INW.IWW} \times \left(T_{IWW}^{t+\Delta t} - T_{INW}^{t+\Delta t}\right) + h_{r-INW.ICW} \times \left(T_{ICW}^{t+\Delta t} - T_{INW}^{t+\Delta t}\right) + h_{r-INW.IHFW} \times \left(T_{s}^{t} - T_{INW}^{t+\Delta t}\right) \quad (11)$$

- **Thermal transfer balance at the external west façade**

$$m_{WW} \times Cp_{WW} \times \frac{dT_{EWW}}{dt} = \sum Q_{abso(EWW)} - \sum Q_{iss(EWW)} \quad (12)$$

and;

$$\frac{m_{WW} \times C_{P_C}}{S_{WW}} \times \frac{T_{EWW}^{t+\Delta t} - T_{EWW}^{t}}{\Delta t} = h_{Conv} \times \left(T_{A1}^{t} - T_{EWW}^{t+\Delta t}\right) + \frac{\lambda_C}{e_{WW}} \times \left(T_{IWW}^{t+\Delta t} - T_{EWW}^{t+\Delta t}\right) + h_{r-HV.EWW} \times \left(T_{HV}^{t} - T_{EWW}^{t+\Delta t}\right) + h_{r-grou.EWW} \times \left(T_{grou}^{t} - T_{EWW}^{t+\Delta t}\right) + \alpha_C \times DTFW \quad (13)$$

- **Thermal transfer balance at the internal ambient of the room**

$$m_{air} \times Cp_{air} \times \frac{dT_{air}}{dt} = \sum Q_{abso(air)} - \sum Q_{iss(air)} \quad (14)$$

and;

$$\frac{m_{air}\times Cp_{air}}{S_{air}}\times\frac{T_{A2}^{t+\Delta t}-T_{A2}^{t}}{\Delta t}=h_{C1}\times\frac{S_{SW}}{S_{air}}\left(T_{ISW}^{t+\Delta t}-T_{A2}^{t+\Delta t}\right)+h_{C2}$$
$$\times\frac{S_{NW}}{S_{air}}\left(T_{INW}^{t+\Delta t}-T_{A2}^{t+\Delta t}\right)+h_{C3}\times\frac{S_{WW}}{S_{air}}\left(T_{IWW}^{t+\Delta t}-T_{A2}^{t+\Delta t}\right)+h_{C4}$$
$$\times\frac{S_{EW}}{S_{air}}\left(T_{IEW}^{t+\Delta t}-T_{A2}^{t+\Delta t}\right)+h_{C5}\times\frac{S_{ICW}}{S_{air}}\left(T_{ICW}^{t+\Delta t}-T_{A2}^{t+\Delta t}\right)+h_{C6} \quad (15)$$
$$\times\frac{S_{IHFW}}{S_{air}}\left(T_{S}^{t+\Delta t}-T_{A2}^{t+\Delta t}\right)+\frac{S_{small}}{S_{air}}\times V_{wind}\times 0.34\times\left(T_{A1}^{t}-T_{A2}^{t+\Delta t}\right)$$
$$+\frac{V_{total}}{S_{air}\times 3600}\times 2\times n_{50}\times\zeta\times\varepsilon\times\left(T_{A1}^{t}-T_{A2}^{t+\Delta t}\right)\times\rho_{air}\times C_{Pair}$$

- **Equation of inertia**

The inertia capacity of a material measures its ability to store heat and postpone its restitution [23]. It is given by the following relation:

$$C_{iner(i)}=\rho_i\times e_i\times S_i\times Cp_i \quad (16)$$

Table 3 Numerical data used for the simulation

Sizes	Values
Soil reflection coefficient	$Albédo = 0.25$
Density of concrete	$\rho_c = 1400 Kg.m^{-3}$
Concrete specific heat	$Cp_c = 1000 J.Kg^{-1}.K^{-1}$
Concrete conductivity	$\lambda_c = 0.51 W.m^{-1}.K^{-1}$
Concrete emissivity	$\varepsilon = 0.91$
Absorption coefficient of concrete	$\alpha_c = 0.55$
Density of air at 25 ° C	$\rho_{air} = 1000 Kg.m^{-3}$
Specific heat of air at 25 ° C	$Cp_{air} = 4182 J.Kg^{-1}.K^{-1}$
Thermal conductivity of air at 25 ° C	$\lambda_{air} = 0.597 W.m^{-1}.K^{-1}$
Dynamic air viscosity at 25 ° C	$\mu_{air} = 10^{-3} Kg.m^{-1}.S^{-1}$
Surface of the small opening for introducing air into the heated space	$S_{small} = 2.10^{-2} m^2$
Air exchange rate for a building with single-glazed window and its joint	$\eta_{50} = 13h^{-1}$
Coefficient of exposure to the wind of the heated room with single exposure for a building in a non-sheltered area	$\zeta = 3.10^{-2}$
Corrective factor of the heated volume height	$\varepsilon_i = 1$

3. Flowchart of the numerical modeling

The procedure adopted for calculating the different temperatures of the outer and inner walls of the habitable enclosure is illustrated by the flowchart of Figure 3. The evaluation of the temperature of each wall is accomplished by following the steps below:

- Importing of climate data for the region;
- Choice of the typical day (in this study: July 17, 2014);
- Introduction of the densities data of the incident solar flux along the five orientations of the facades;
- Introduction of the geometric parameters of the habitable enclosure;
- Introduction of the physical and thermal properties of building materials;
- Introduction of other parameters, such as, the Boltzmann constant, soil temperature, mean wind speed, heating floor temperature and time step;
- Determination of the geometric shape factors of the habitat;
- Calculation of the thermal exchange coefficients by convection, conduction and radiation;
- Evaluation of all internal and external temperatures of the habitable enclosure walls;

It should be noted that with the implicit schema of finite differences, the tests that we carried out, during the development of the computational program, led us to retain a time step of 300s.

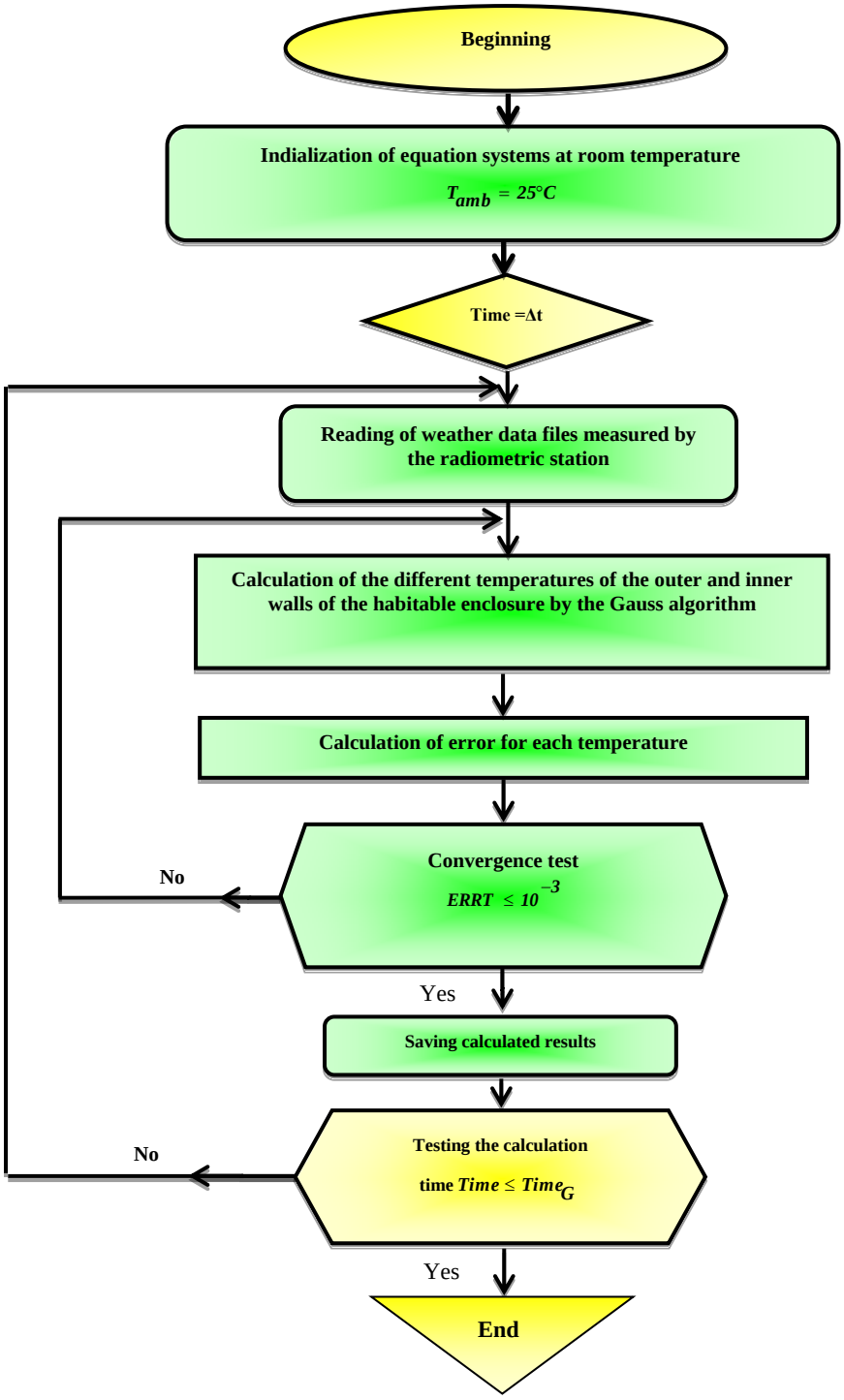

Figure 3 Flowchart of the numerical modeling.

4. Results and discussion

4.1. Validation

In order to validate the results obtained by the developed model, in what follows, we compare the values obtained by the computational code with that measured by the Adrar radiometric station during the typical day of 17 July 2014. Tables 4 and 5 shows respectively the values of the computed densities of the global and direct solar fluxes incident on a horizontal plane in comparison with those

of experimental data. It may be noted that there is an acceptable difference between the computed and experimentally measured results. Indeed, the average relative difference is of 37.15% for the case of the global solar flux and of 29.8% for the case of the direct solar flux.

Table 4 Comparison of the numerical results and the experimental data in the case of the density of the total solar flux incident on a horizontal plane.

Time (h)	**Density of the total flux calculated in (W/m^2)**	**Density of the total flux measured in (W/m^2)**	**Relative error of the global flux density**	**Average error of the global flux density**
1	0	0	0	
2	0	0	0	
3	0	0	0	
4	0	0	0	
5	0	0	0	
6	0	10	1	
7	233,8695	118	0,981944915	
8	456,01181	354	0,288168955	
9	655,28778	562	0,165992491	
10	821,70489	759	0,082615138	
11	946,91828	893	0,060378813	
12	1024,64924	999	0,025674915	0,37150243
13	1051	1038	0,012524085	
14	1024,64924	996	0,028764297	
15	946,91828	904	0,047475973	
16	821,70489	800	0,027131113	
17	655,28778	600	0,0921463	
18	456,01181	400	0,140029525	
19	233,8695	72	2,2481875	
20	0	0	0	
21	0	0	0	
22	0	0	0	
23	0	0	0	
24	0	0	0	

Table 5 Comparison of the numerical results and experimental data in the case of the density of the density of the direct incident solar flux on a horizontal plane.

Time (h)	Density of the direct flux calculated in (W/m^2)	Density of the direct flux measured in (W/m^2)	Relative error of the direct flux density	Average error of the direct flux density
1	0	0	0	
2	0	0	0	
3	0	0	0	
4	0	0	0	
5	0	0	0	
6	0	3	1	
7	215,04376	85	1,529926588	
8	427,56561	366	0,168212049	
9	619,4466	600	0,032411	
10	780,58133	750	0,040775107	
11	902,29676	810	0,113946617	
12	978,03974	899	0,087919622	0,298943706
13	1003,74612	970	0,034789814	
14	978,03974	975	0,003117682	
15	902,29676	850	0,0615256	
16	780,58133	680	0,147913721	
17	619,4466	600	0,032411	
18	427,56561	380	0,125172658	
19	215,04376	119	0,80709042	
20	0		0	
21	0		0	
22	0		0	
23	0		0	
24	0		0	

4.2 Evolution of internal and external ambient temperatures

Figure 4 shows the evolution of daily temperatures of the external facades of the habitable enclosure during the selected typical day. It can be seen that there is a noticeable phase shift between the external ambient temperature and the other temperatures of the outer facades. This phase shift can be attributed to the thermal inertia and its cruel effects on the thermal behavior of the habitable enclosure walls. In addition, these effects are more pronounced especially during the daytime period when the temperature of the horizontal face is greater with respect to the others. Indeed, it makes a phase shift of one hour thirty minutes in comparison with the external ambient temperature.

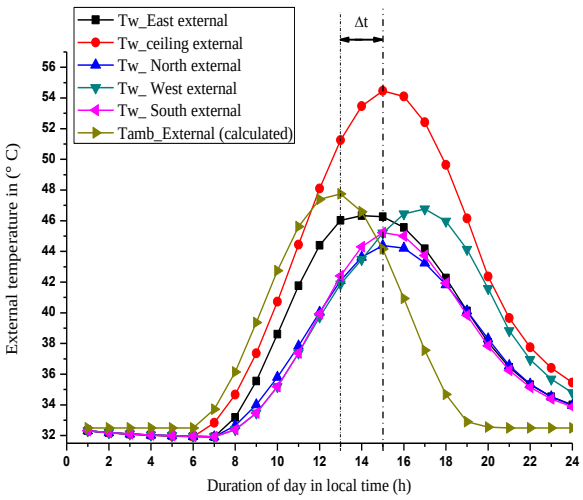

Figure 4 Variation of the temperature of the enclosure external walls as a function of local time.

Figure 5 shows the variation of the internal faces temperature of the habitable enclosure during the selected typical day. It can be seen that the thermal inertia of the concrete plays an important role in the conductive thermal transfer of the walls. Indeed, the temperature of the bottom ceiling is greater than the temperatures of the other internal faces (i.e., South, West, North and East faces). This is due to two essential factors that are combined to generate this temperature increase. Firstly, the thickness of the habitat walls, which involves the increase of thermal inertia, and secondly, the incidence angle of the sun's rays which is equal to 0 °.

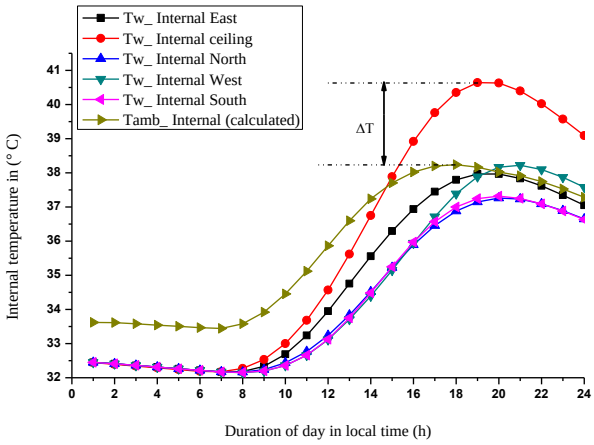

Figure 5 Variation of the temperature of the enclosure internal walls as a function of local time.

4.3. Evolution of the internal temperature of the enclosure

The evolution of the internal ambient temperature of the habitable enclosure as a function of the local time for different temperatures of the heating slab is shown in figure 6. It may be noted that as the temperature of the heating slab increases, the internal temperature of the enclosure increases in a systematic manner during the diurnal period. From a physical point of view, there is a 5-hour phase shift between the external and internal ambient temperatures.

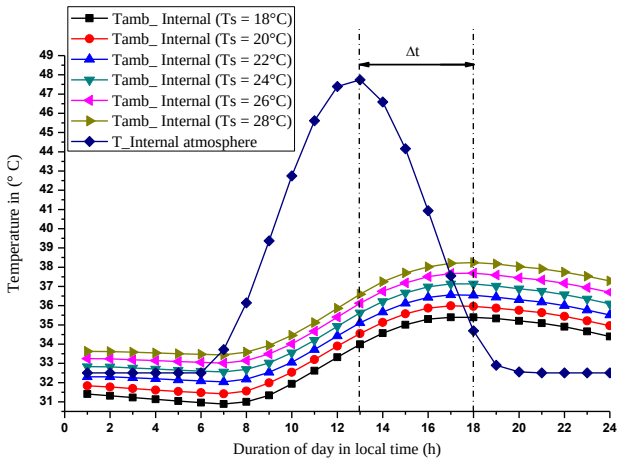

Figure 6 Evolution of the internal ambient temperature as a function of the local time for different temperatures of the heating slab.

Figure 7 illustrates the evolution of the internal ambient temperature as a function of the local time for different walls thicknesses of the habitable enclosure. It can be seen that if the thickness of the concrete increases, the internal temperature of the enclosure decreases, and vice versa. Indeed, this variation in the internal temperature is due to the fact that the thermal inertia of the concrete plays a significant role in the thermal exchanges which take place within the habitable enclosure.

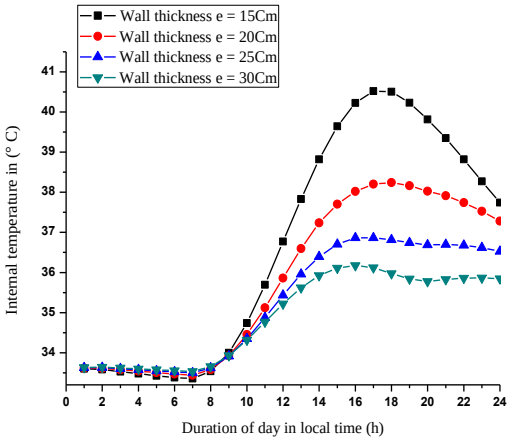

Figure 7 Evolution of the internal ambient temperature as a function of the local time for different thicknesses of the walls.

It is interesting to note that the wind contributes to the renewal of air in the housing by natural ventilation, which is reflected in the degree of leakage of the enclosure envelope (quality of the windows and doors joints). In figure (8.a) which shows the degree of sealing effect of the windows and doors, it can be seen that before 18 hours, namely in the diurnal period, the habitable enclosure with normal quality and even in the case where there are no joints, the ambient temperature reaches a maximum value of 38°C. However, for the same enclosure with high-quality joints, the maximum internal ambient temperature is 37 °C. This slight difference is due to both the permeability of the windows and the doors and the external ambient temperature which is very high in July. Whereas, in the case of the night period (after 18 pm), we found the reverse.

It should be noted that the wind pressure on the building constitutes the predominant boundary conditions in the evaluation of air flows. In order to study its effect on the thermal comfort, it is important to adapt the available data (wind speed and orientation measured at a meteorological station) to the characteristics of the site (presence of obstacles such as trees, neighboring buildings,

etc.). Figure (8.b) shows the wind coefficient effect on the habitable enclosure for different possibilities, such as a building without facade exposed to the wind, a building with one facade exposed to the wind and a building with multiple facades exposed to the wind. It can be noted that by increasing the coefficient of exposure to wind the temperature of the heated space increases significantly between the interval of 0.01 to 0.02, however between 0.02 and 0.03 a slight difference has been observed. This explains that the higher the coefficient of wind exposure (between 0.02 and 0.03), the closer the temperature of the heated space is to the external ambient temperature.

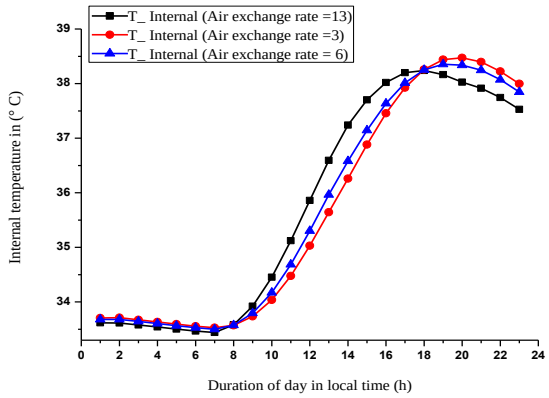

(a)

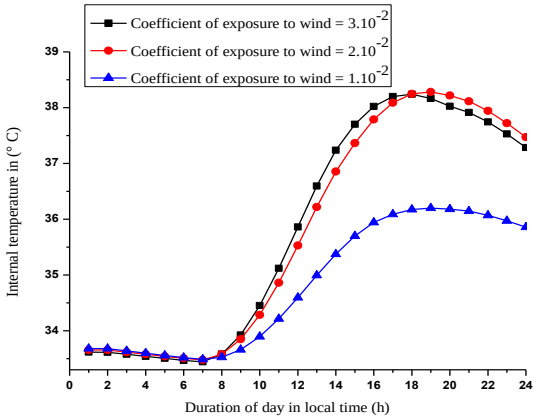

(b)

Figure 8 Variation of the internal temperature according to: (a) the quality of the sealing and (b) the coefficient of exposure to the wind for the habitable enclosure.

5. Conclusion

The use of solar energy in the building is a promoter topic of research in Algeria which has a considerable solar energy potential and especially in the region of ADRAR. The study presented in this paper shows that the developed model can be used for the prediction of the thermal behavior inside and outside of a habitable enclosure located in a desert region. Indeed, we have analyzed the effects of several parameters on the thermal comfort, such as, incident solar flux, external temperature, wall thickness, wind exposure coefficient and the quality of sealing.

The results show that in the diurnal period the interior temperature of the habitable enclosure with several facades exposed to the wind and with a high-quality sealing is moderately lower than that of an enclosure with a simple facade exposed to the wind and a low degree of sealing. Therefore, to improve the comfort level inside the living area, the joints must be of high-quality and the wind

exposure coefficient must be reduced to the maximum possible as the external ambient temperature in this region is very high during the month of July.

It is noticed that the high thermal inertia of the building material used for the habitable enclosure has a considerable effect on the stabilization of the thermal comfort. Thus, it is advised to use other materials with low thermal inertia in the construction, such as, clay-based materials.

Moreover, the increase in the temperature of the heating slab leads to an increase of the internal temperature and, consequently, to an undesirable overheating of the envelope. For this reason, it is necessary to respect the ISO standards that govern the permissible limits of the heating slab temperature.

Acknowledgements

I would especially like to thank my supervisor, Professor AOUR BENOUMUER, the director of the Laboratory of Applied Biomechanics and Biomaterials "LABAB" for their many readings and corrections of my disastrous English. They have always responded, even in the most desperate cases. I thank Professor ZEGHMATI BELKACEM for co-supervising this work of finalization of my thesis. He initially allowed me to integrate the image team by offering me a very interesting subject and left me the freedom to re-orient it during the course of my thesis. It was also thanks to his collaboration with the laboratory " LAMPS " at the University of Perpignan, that I had the chance to work with Professor CHESNEAU XAVIER, which proved to be a very enriching experience. During this work, he often drew my attention to some design problems and spent a lot of time, among other things to deal with my obstacles in my numerical simulation code.

I would particularly like to thank Professor MESSAOUD HAMOUDA the Director of the ADRAR Renewable Energy Research Unit (URER.MS) for their sympathy and efficiency in organizing and solving administrative problems concerning the recent climatic data of the region of Adrar for the year 2014.

References

[1] I. Traore, Transferts de chaleur et de masse dans les parois des bâtiments à ossature bois, Thèse de doctorat de l'Université Henri Poincaré – Nancy Université en Mécanique et Energétique, 2011, ch. 1.

[2] G. Lefebvre, Comportement thermique dynamique des bâtiments: simulation et analyse, Techniques de l'Ingénieur, traité Génie énergétique, Paris-CENERG, B 2 041-1, pp.9-10.

[3] S. Jiang, C. Grey, Wouter Poortinga and Chris Tweed, "Winter Indoor Air Temperature and Relative Humidity in Hard-To-Heat, Hard-To-Treat Houses in Wales: Results from a Household Monitoring Study'', WSA Working Paper Series, ISSN 2050-8522, pp. 05-48, March 2015.

[4] S. Ferrari, V. Zanotto, "The thermal performance of walls under actual service conditions: Evaluating the results of climatic chamber test'', Construction and Building Materials, vol. 43, pp. 309-316, February 2013.

[5] E. Wurtz, Modélisation tridimensionnelle des transferts thermiques et aérauliques dans le bâtiment en environnement orienté objet, Thèse de doctorat Ecole Nationale des Ponts et Chaussees, 2010, ch.1.

[6] M. Papalardo, Amélioration énergétique des bâtiments existants, ADEME Editions et Fédération Française du Bâtiment, 1 vol., 2004, pp.27-107.

[7] J. Berger, Contribution à la modélisation hygrothermique des bâtiments: Application des méthodes de réduction de modèle, Thèse de docteur de l'université de Grenoble, Spécialité: Génie Civil et Sciences de l'Habitat, 2014, Ch.1.

[8] M. Madaci, D. Kerdoun, ‘’Case Study of a Solar Pumped Storage Prototype Station Implementation Designed for the Region of Ghardia’’, International journal of renewable energy research, vol.6 (2), pp.435-446, May 2016.

[9] H. Othieno, J. Awange, Energy resources in Africa: Distribution, Opportunities and Challenge, Springer International Publishing, Switzirland, 2016, pp.193-221.

[10] S. Bentouba, “L’énergie renouvelable en Algérie et l’impact sur l’environnement”, Journal of Scientific Research, Université de Bechar, vol. 1, pp.50-54, November, 2010.

[11] K.A., Antonopoulos E. Koronaki, "Apparent and effective thermal capacitance of buildings", Energy, vol. 23 (3), pp.183-192, March 1998.

[12] F. Sebaa, Etude du potentiel éolien d’Adrar Sélection de sites pour la ferme éolienne de 10 MW, Revue des Energies Renouvelables, pp. 295-300, April 2010.

[13] ENERMENA High Precision Meteorological Station of Research Unit for Renewable Energies in the Saharan Environment in ADRAR, Algeria, 2014.

[14] A. Oudrane, B. Aour, M. Benhamou, ‘’Analyse de l’effet de l’épaisseur de la dalle chauffante sur l’effecacité thermique d’une installation de plancher solaire direct (PSD) implantée à ADRAR’’, African Review of Science, Technology and Development, vol. 01(01), pp. 26-41, January 2016.

[15] A. Oudrane, B. Aour, M. Hamouda, M. Benhamou, ‘’Méthodologie pour la détermination de l’écartement optimal de la chaine tubulaire d’une dalle chauffante’’, Revue des Energies Renouvelables, vol. 19(01), pp. 11-19, Mars, 2016.

[16] S. Bekkouche, T. Benouaz and A. Cheknane, ‘’A modelling Approach of Thermal Insulation Applied to a Saharan Building’’, Thermal Science, No. 4, vol. 13, pp. 233-244, October 2009.

[17] Liu, B.Y.H and Jordan, R.C., “The interrelationship and characteristics distribution of direct, diffuse and total solar radiation”. Solar Energy. 4(3). pp.1-19, July,1960.

[18] G.S. Campbell, J.M. Norman, An Introduction to Environmental Biophysics, 2nd Edition, Springer Verlag, Berlin, Heidelberg, New York Journal of Plant Physiology, Volume 155, Issue2, 1999, Page 296, August, 1998.

[19] A. Oudrane, B. Zeghmati, X. Chesneau, B. Aour B., ‘’Modélisation du bilan radiatif et énergetique d’un habitat situé dans la region d’ADRAR’’, Recueil de Mécanique, vol. 2, pp. 79-87, Févier 2016.

[20] K. Mansatiansin, Modélisation et simulation des transferts et de l’éclairement dans un habitat bioclimatique, Thèse de doctorat en sciences de l’ingénieur, spécialité mécanique énergétique, Université de Perpignan, 2005, ch.2.

[21] D.M. Whaley, W.Y. Saman, A.T. Alemu, ‘’Integrated Solar Thermal System for Water and Space Heating, Dehumidification and Cooling’’, Energy Procedia Vol.57, pp. 2590 – 2599, October 2014.

[22] M. Daguenet, Les Séchoirs Solaires, Théorie et Pratique, Editions Unesco, Paris, 1985, pp. 81-106.

[23] N. Boulfaf, J. Chaoufi, A. Ghafiri, A. Elorf, ‘’Thermal Study of Hybrid Photovoltaic Thermal (PV-T) Solar Air Collector Using Finite Element Method’’, International Journal of Renewable Energy Research, Vol. 6(1), pp. 171-182, February 2016.

[24] M. Boukli, ‘’Thermal requirements and temperatures evolution in an ecological house’’, Energy Procedia, vol. 6, pp. 110-121, December 2011.

[25] S. Robelison, ‘’Influence thermique de l’emplacement du toit en chaume sous le toit en tôle d’un habitat à Antananarivo-Madagascar’’, Afrique SCIENCE, vol.04(3), pp. 318-338, ISSN 1813-548X, 2008.